RESEARCH
Open Access

Average bit error probability for the λ-MRC detector under Rayleigh fading

Mitchell Omar Calderon Inga and Gustavo Fraidenraich[*]

Abstract

In this paper, an exact expression for the average bit error probability was obtained for the λ-MRC detector, proposed in Sendonaris et al. (IEEE Trans Commun 51: 1927-1938, IEEE Trans. Commun 51: 1939-1948), under Rayleigh fading channel. In addition, a very accurate approximation was obtained to calculate the average bit error probability for any power allocation scheme. Our expressions allow to investigate the possible gains and situations where cooperation can be beneficial.

Keywords: User cooperation, Virtual MIMO, Bit error probability, Rayleigh fading

I. Introduction

Diversity techniques have been widely accepted as one of effective ways of combat multipath fading in wireless communications [1], in particular spatial diversity is specially effective at mitigating these multipath situation. However, in many wireless applications, the use of multiple antennas is not practical due to size and cost limitations of the terminals. One possible way to have diversity without increasing the number of antennas is through the use of cooperative diversity.

Cooperative diversity has root in classical information theory work on relay channels [2], [3]. Cooperative networks achieve diversity gain by allowing the users to cooperate, and thus, each wireless user is assumed to transmit data as well as act as a cooperative agent for another user [4], [5]. The first implementation strategy for cooperation was introduced in [1], [6], where the achievable rate region, outage probability, and coverage area were analyzed.

In this pioneering work, assuming a suboptimal receiver called λ-MRC, the bit error probability was computed assuming a fixed channel. This kind of receiver combines the signal from the first period of transmission with the signal transmitted jointly by the both users in the second period of transmission. The variable λ ∈ [0,1] establishes the degree of confidence in the bits estimated by the partner. For situations where the inter-user channel presents favorable conditions, the variable

λ should be close to unity; on the other hand, for very severe channels conditions, the parameter λ should tend to zero. Unfortunately, the bit error probability was computed only for a fixed channel and remained open for the situation where all the fading coefficients are Rayleigh distributed.

In this paper, an exact and approximate expression is computed for the average bit error probability assuming a Rayleigh fading for the inter-user channel and for the direct channel between users and base station (BS).

II. System Model

This section summarizes the system model that was employed in [1], [6].

A. System Model

The channel model used in [6] can be mathematically expressed as

$$Y_0(t) = K_{10}X_1(t) + K_{20}X_2(t) + Z_0(t) \tag{1}$$

$$Y_1(t) = K_{21}X_2(t) + Z_1(t) \tag{2}$$

$$Y_2(t) = K_{12}X_1(t) + Z_2(t) \tag{3}$$

where $Y_0(t)$, $Y_1(t)$, and $Y_2(t)$ are the baseband models of the received signal at the BS, user 1, and user 2, respectively, during one symbol period. Also, $X_i(t)$ is the signal transmitted by user i under power constraint P_i, for $i = 1, 2$, and $Z_i(t)$ are white zero-mean Gaussian noise random processes with spectral height $\mathcal{N}_i/2$ for i

* Correspondence: gf@decom.fee.unicamp.br
Department of Communications, University of Campinas, Campinas, Brazil

= 0, 1, 2, and the fading coefficients K_{ij} are Rayleigh distributed with $E\left[K_{ij}^2\right] = 2\alpha_{ij}^2$. We also assume that the BS can track perfectly the variations in K_{10} and K_{20}, user 1 can track K_{21} and user 2 can track K_{12}.

The system proposed in [6] is based on a conventional code division multiple access (CDMA) system and divides the transmission into two parts: the first without cooperation and the second with cooperation. For a given coherence time of L symbols and cooperation time of $2L_c$ symbols, the transmitted signals can be expressed as shown in (5), where $L_n = L-2L_c$, $b_j^{(i)}$ is user j's ith bit, $\hat{b}_j^{(i)}$ is the partner's estimate of user j's ith bit, and $c_j(t)$ is user j's spreading code. The parameters a_{ij} represent the power allocation scheme, and they must maintain an average power constraint that can be expressed as

$$
\begin{aligned}
\frac{1}{L}\left(L_n a_{11}^2 + L_c\left(a_{12}^2 + a_{13}^2 + a_{14}^2\right)\right) &= P_1 \\
\frac{1}{L}\left(L_n a_{21}^2 + L_c\left(a_{22}^2 + a_{13}^2 + a_{14}^2\right)\right) &= P_2
\end{aligned}
\tag{4}
$$

$$
X_1(t) = \begin{cases}
a_{11}b_1^{(i)}c_1(t), & i = 1, 2, \ldots, L_n \\
a_{12}b_1^{(L_n+1+i)/2}c_1(t), & i = L_n+1, L_n+3, \ldots, L-1 \\
a_{13}b_1^{(L_n+i)/2}c_1(t) + a_{14}\hat{b}_2^{(L_n+i)/2}c_2(t), & i = L_n+2, L_n+4, \ldots, L
\end{cases}
$$
$$
X_2(t) = \begin{cases}
a_{21}b_2^{(i)}c_2(t), & i = 1, 2, \ldots, L_n \\
a_{22}b_2^{(L_n+1+i)/2}c_2(t), & i = L_n+1, L_n+3, \ldots, L-1 \\
a_{23}\hat{b}_1^{(L_n+i)/2}c_1(t) + a_{24}b_2^{(L_n+i)/2}c_2(t), & i = L_n+2, L_n+4, \ldots, L
\end{cases}
\tag{5}
$$

In the first $L_n = L - 2L_c$ symbol periods, each user transmits its own bits to the BS. The remaining $2L_c$ periods are dedicated to cooperation: odd periods for transmitting its bits to both the partner and the BS; even periods for transmitting a linear combination of its own bit and the partner's bit estimate.

B. Error Calculations

1) Error Rate for Cooperative Periods: During the $2L_c$ cooperative periods, we have a distinction between "odd" and "even" periods. During the "odds" periods, each user sends only their own bit, which is received and detected by the partner as well as by the BS.

The partner's hard estimate of b_1 is given by $\hat{b}_1 = \text{sign}\left((1/N_c)c_1^TY_2\right)$, resulting in a probability of bit error equals to

$$
P_{e_{12}} = Q\left(K_{12}a_{12}\frac{\sqrt{N_c}}{\sigma_2}\right)
\tag{6}
$$

where $Q(\cdot)$ is the Gaussian error integral, N_c is the CDMA spreading gain, $\sigma_2^2 = \mathcal{N}_2/(2T_c)$, T_c is the chip period, and $\mathcal{N}_2/2$ is the spectral height of $Z_2(t)$.

The BS forms a soft decision statistic by calculating

$$
\gamma_{\text{odd}} = \frac{1}{N_c}c_1^TY_0^{\text{odd}}
\tag{7}
$$

where $Y_0^{\text{odd}} = K_{10}X_1 + K_{20}X_2 + Z_0^{\text{odd}}$.

During the "even" periods, each user send a cooperative signal to BS according to $Y_0^{\text{even}} = K_{10}X_1 + K_{20}X_2 + Z_0^{\text{even}}$, and the BS extracts a soft decision statistic by calculating

$$
\gamma_{\text{even}} = \frac{1}{N_c}c_1^TY_0^{\text{even}}
\tag{8}
$$

The combined statistics at BS for user 1 is therefore given by

$$
\begin{aligned}
\gamma_{\text{odd}} &= K_{10}a_{12}b_1 + n_{\text{odd}} \\
\gamma_{\text{even}} &= K_{10}a_{13}b_1 + K_{20}a_{23}\hat{b}_1 + n_{\text{even}}
\end{aligned}
\tag{9}
$$

where n_{odd} and n_{even} are statistically independent and both distributed according to a Gaussian distribution $\mathcal{N}(0, \sigma_0^2/N_c)$.

The optimal detector shown in [1] is rather complex and does not have a closed-form expression for the resulting bit error probability. Thus, they consider the following suboptimum detector

$$
\hat{b}_1 = \text{sign}\left([K_{10}a_{12} \ \lambda(K_{10}a_{13} + K_{20}a_{23})]y\right)
\tag{10}
$$

where $y = [\gamma_{\text{odd}} \ \gamma_{\text{even}}]^T \sqrt{N_c}/\sigma_0$ and $\lambda \in [0,1]$. They call this suboptimum detector as the λ-MRC. The probability of bit error for this detector is given by

$$
P_{e_1} = (1 - P_{e_{12}})Q\left(\frac{v_\lambda^T v_1}{\sqrt{v_\lambda^T v_\lambda}}\right) + P_{e_{12}}Q\left(\frac{v_\lambda^T v_2}{\sqrt{v_\lambda^T v_\lambda}}\right)
\tag{11}
$$

where

$v_\lambda = [K_{10}a_{12} \ \lambda(K_{10}a_{13} + K_{20}a_{23})]^T$, $v_1 = [K_{10}a_{12} \ \lambda(K_{10}a_{13} + K_{20}a_{23})]^T \ \sqrt{N_c}/\sigma_0$
and $v_2 = [K_{10}a_{12} \ (K_{10}a_{13} - K_{20}a_{23})]^T \ \sqrt{N_c}/\sigma_0$.

III. Rayleigh fading calculations

The expression presented in (11) is only valid for a fixed (time-invariant) channel, that is, the fading coefficients K_{ij} are fixed. The aim of this paper is to obtain an expression for the bit error probability when the fading coefficients vary according to a Rayleigh distribution.

A. Bit Error Probability

The bit error probability associated with the signal from user 1, at user 2, for a fixed gain is described in (6). Now assuming a nonstatic situation, the average bit error probability can be computed averaging (6) with respect to a Rayleigh distribution

$$\bar{P}_{e_{12}} = E[P_{e_{12}}] = \frac{1}{2}\left(1 - \sqrt{\frac{\gamma_{12}}{2+\gamma_{12}}}\right) \tag{12}$$

where γ_{12} is the average signal-to-noise ratio, defined as

$$\gamma_{12} = \frac{2a_{12}^2\alpha_{12}^2 N_c}{\sigma_2^2} \tag{13}$$

From (11), we can define two random variables U_1 and U_2, respectively, as

$$\frac{v_\lambda^T v_1}{\sqrt{v_\lambda^T v_\lambda}} = \sqrt{U_1} = \frac{\left((K_{10}a_{12})^2 + \lambda(K_{10}a_{13} + K_{20}a_{23})^2\right)\sqrt{N_c}}{\left((K_{10}a_{12})^2 + \lambda^2(K_{10}a_{13} + K_{20}a_{23})^2\right)\sigma_0} \tag{14}$$

$$\frac{v_\lambda^T v_2}{\sqrt{v_\lambda^T v_\lambda}} = \sqrt{U_2} = \frac{\left((K_{10}a_{12})^2 + \lambda\left((K_{10}a_{13})^2 - (K_{20}a_{23})^2\right)\right)\sqrt{N_c}}{\left((K_{10}a_{12})^2 + \lambda^2(K_{10}a_{13} + K_{20}a_{23})^2\right)\sigma_0} \tag{15}$$

since K_{10} and K_{20} are Rayleigh distributed, the support of (14) will be always greater than zero. On the other hand, since we have negative values in the numerator of (15), its support will be all the real line. Taking this into account, we can rewrite (11) as

$$P_{e_1} = \left(1 - P_{e_{12}}\right)Q\left(\sqrt{U_1}\right) + P_{e_{12}}Q(U_2) \tag{16}$$

To obtain the error probability, we must average P_{e_1}, over the probability density function (PDF) of U_1 and U_2 [7]. Thus, we have to evaluate the integral

$$P_{e_f} = \left(1 - \bar{P}_{e_{12}}\right)\int_0^\infty Q\left(\sqrt{u_1}\right)f_{u_1}(u_1)du_1 + \\ \bar{P}_{e_{12}}\int_{-\infty}^\infty Q(u_2)f_{u_2}(u_2)du_2 \tag{17}$$

In order to calculate P_{ef}, we have to know the distribution of U_1 and U_2, thus to facilitate the calculations, we assume an equal power allocation situation, where $a_{12} = a_{13} = a_{23} = a$. With this assumption the random variables U_1 and U_2 will be simplified to

$$U_1 = \frac{a^2\left(K_{10}^2 + \lambda(K_{10} + K_{20})^2\right)N_c}{\left(K_{10}^2 + \lambda^2(K_{10} + K_{20})^2\right)\sigma_0^2} \tag{18}$$

$$U_2 = \frac{a\left(K_{10}^2 + \lambda\left(K_{10}^2 + K_{20}^2\right)\right)\sqrt{N_c}}{\left(\sqrt{K_{10}^2 + \lambda^2(K_{10} + K_{20})^2}\right)\sigma_0} \tag{19}$$

Since U_1 depends on K_{10} and K_{20}, it is possible to write the cumulative distribution function (CDF) and the PDF of U_1, respectively, as

$$F_{u_1}(u_1) = \int\int_{k_{10},k_{20}\in D_{u_1}} f_{u_1}(k_{10},k_{20})dk_{10}dk20 \tag{20}$$

$$f_{u_1}(u_1) = \frac{dF_{u_1}(u_1)}{du_1} \tag{21}$$

In this case, D_{u_1} is the region of the $K_{10} \times K_{20}$ plane where

$$\frac{a^2\left(k_{10}^2 + \lambda(k_{10} + k_{20})^2\right)N_c}{\left(k_{10}^2 + \lambda^2(k_{10} + k_{20})^2\right)\sigma_0^2} \leq u_1 \tag{22}$$

Note that this region is very similar to a rotated ellipse but not exactly an ellipse.

Since K_{10} and K_{20} are independent Rayleigh distribution with parameters α_{10} and α_{20}, respectively, we have

$$F_{u_1}(u_1) = \int_{k_{10}=0}^{a(u_1)}\int_{k_{20}=0}^{b(u_1)} f_{k_{10}k_{20}}(k_{10},k_{20})dk_{20}dk_{10} \tag{23}$$

where

$$a(u_1) = \frac{1}{\lambda_1}\sqrt{\frac{u_1\lambda_2}{A_1}} \tag{24}$$

$$b(u_1) = \frac{\sqrt{2A_1\left(B_1 - \left(2A_1k_{10}^2 - u_1\right)\lambda\right)} - 2A_1k_{10}\lambda^2}{2A_1\lambda} \tag{25}$$

$$A_1 = \frac{a^2 N_c}{\sigma_0^2} \tag{26}$$

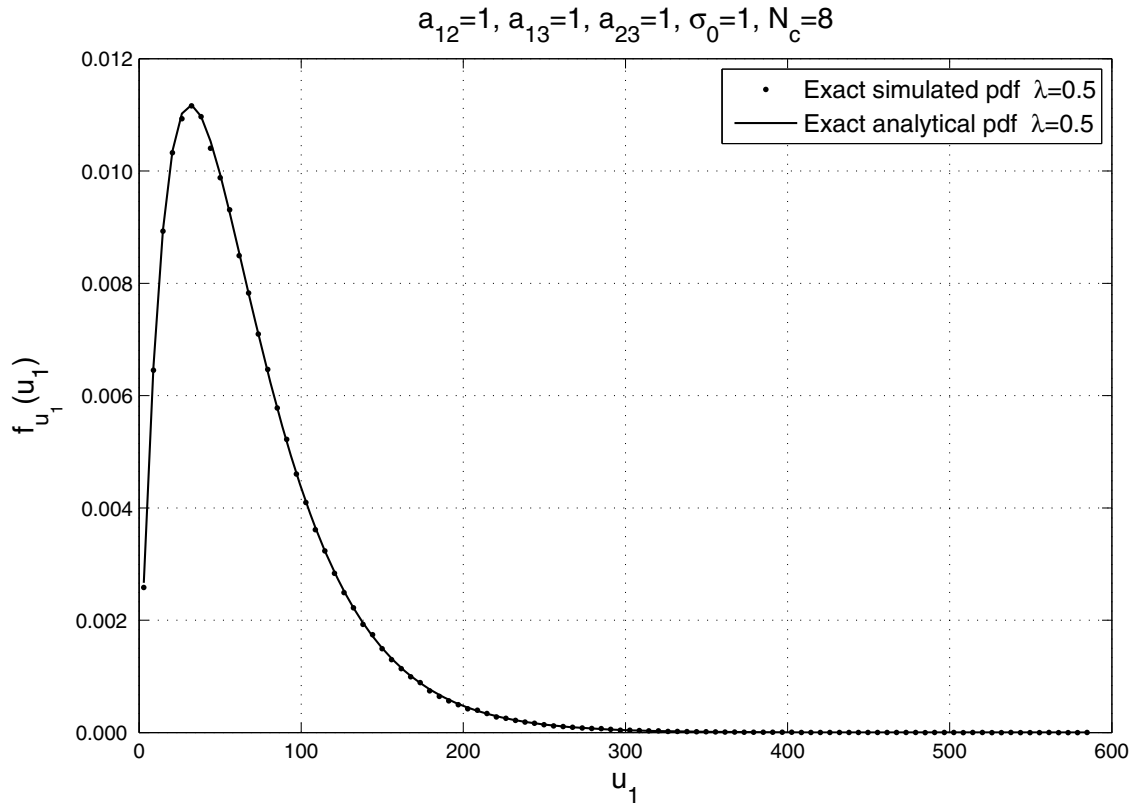$$B_1 = \lambda\sqrt{u_1\left(u_1\lambda^2 - 4A_1k_{10}^2(\lambda - 1)\right)} \tag{27}$$

now it is possible to derive the PDF of U_1 easily as

$$f_{u_1}(u_1) = \int_{k_{10}=0}^{a(u_1)} \frac{\partial b(u_1)}{\partial u_1}\frac{b(u_1)}{\alpha_{20}^2}e^{-\frac{b(u_1)^2}{2\alpha_{20}^2}}\frac{k_{10}}{\alpha_{10}^2}e^{-\frac{k_{10}^2}{2\alpha_{10}^2}}dk_{10} \tag{28}$$

and unfortunately, it is not possible to evaluate (28) in a closed-form solution.

In order to validate the above formulation, Figure 1 shows the analytical and simulated PDF of U_1. Note the excellent agreement between them showing the correctness of our formulation.

Following similar rationale, we now find the CDF and PDF of U_2. Note that in this case, the region of integration, D_{u_2}, will be given by

Figure 1 Comparison between analytical and simulated PDF for U_1

$$\frac{a\left(k_{10}^2 + \lambda\left(k_{10}^2 - k_{20}^2\right)\right)\sqrt{N_c}}{\left(\sqrt{k_{10}^2 + \lambda^2(k_{10}+k_{20})^2}\right)\sigma_0} \leq u_2 \tag{29}$$

leading to the following CDF and PDF, respectively, as

$$F_{u_2}(u_2) = \begin{cases} \int\limits_{k_{20}=\frac{|u_2|}{A_2}}^{\infty} \int\limits_{k_{10}=0}^{\infty} f_{k_{10}k_{20}}(k_{10},k_{20})\,dk_{10}dk_{20} & \text{if } u_2 < 0, \\ \int\limits_{k_{20}=0}^{\infty} \int\limits_{k_{10}=0}^{a(u_2)} f_{k_{10}k_{20}}(k_{10},k_{20})\,dk_{10}dk_{20} & \text{if } u_2 \geq 0. \end{cases} \tag{30}$$

and

$$f_{u_2}(u_2) = \begin{cases} \int\limits_{\frac{|u_2|}{A_2}}^{\infty} \frac{\partial b(u_2)}{\partial u_2} f_{k_{10}k_{20}}(b(u_2),k_{20})dk_{20} & \text{if } u_2 < 0, \\ \int\limits_{0}^{\infty} \frac{\partial a(u_2)}{\partial u_2} f_{k_{10}k_{20}}(a(u_2),k_{20})dk_{20} & \text{if } u_2 \geq 0. \end{cases} \tag{31}$$

where

$$a(u_2) = \Re\left(\frac{1}{2A_2\lambda_1\sqrt{3}}\left(\sqrt{R_1}+\sqrt{\frac{R_2}{2}}\right)\right) \tag{32}$$
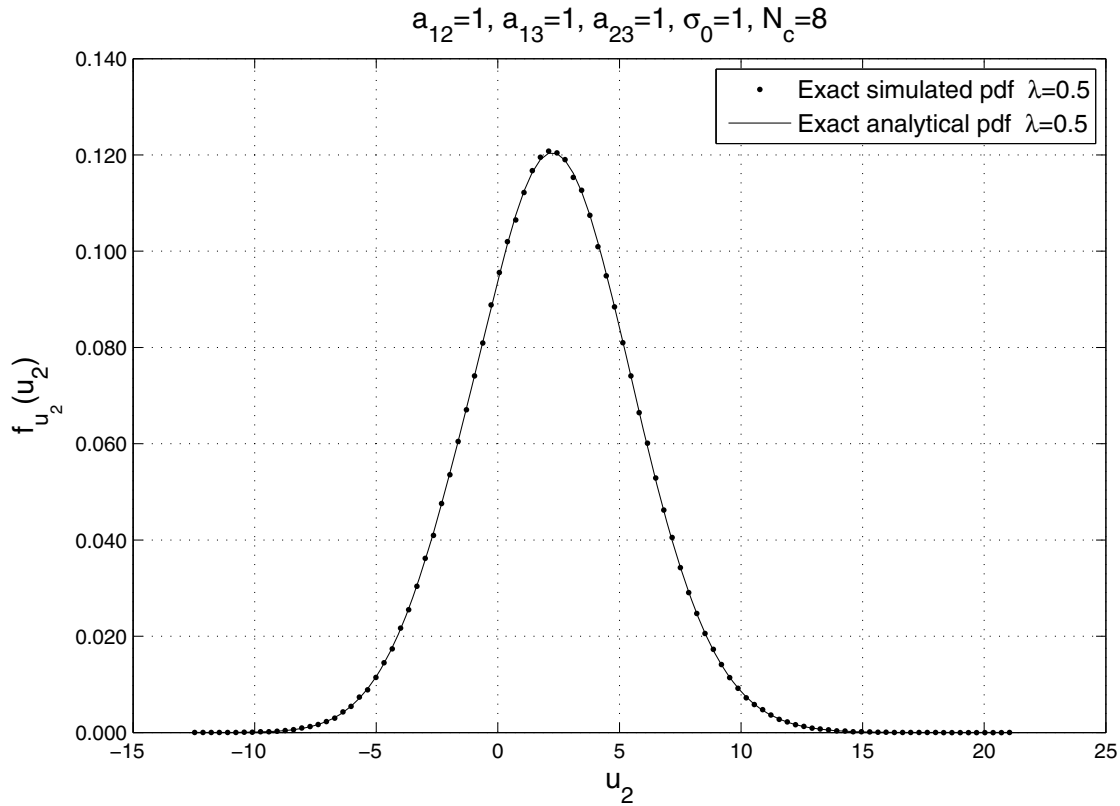
$$b(u_2) = \Re\left(\frac{1}{2A_2\lambda_1\sqrt{3}}\left(\sqrt{R_1}+\sqrt{\frac{R_2}{2}}\right)\right) \tag{33}$$

$$A_2 = \frac{a\sqrt{N_c}}{\sigma_0} \tag{34}$$

where $\Re(\cdot)$ denotes the real part of a number, and R_1 and R_2 are described in the Appendix.

In the same way as in the first case, (31) cannot be obtained in a closed-form solution. Figure 2 compares the analytical and simulated PDF of U_2 in order to validate our formulation.

Once that the PDFs of U_1 and U_2 were exactly computed, it is possible to obtain the average bit error probability by simply substituting (28) and (31) into (17). Figure 3 shows the simulation result of the bit error probability and the result of our theoretical expression given in (17), where we can observe that both curves are almost coincident. In this figure, SNR $= \dfrac{P}{\sigma_0^2}$. According to Section II-B, we consider three symbols periods, each period with an average power of P. Also, for simplicity,

Figure 2 Comparison between the exact and simulated PDF for U_2.

we consider that $E\left[K_{10}^2\right]$, $E\left[K_{20}^2\right]$ and $E\left[K_{12}^2\right]$ are identical.

Although (17) presents the exact solution to the average bit error probability, in some cases, the complexity to compute this expression can be prohibitive. For this reason, we found a very accurate approximation for the bit error probability presented in the sequel.

B. Approximate Bit error Probability
The main problem in order to obtain a simpler expression for the bit error probability is to simplify the PDFs of U_1 and U_2 given, respectively, in (14) and (15). In order to obtain an approximation, the expressions (14) and (15) can be reduced when $\lambda = 1$, $\sigma_0 = 1$ and $a_{12} = a_{13} = a_{23} = 1$. Therefore, the new random variables are given by
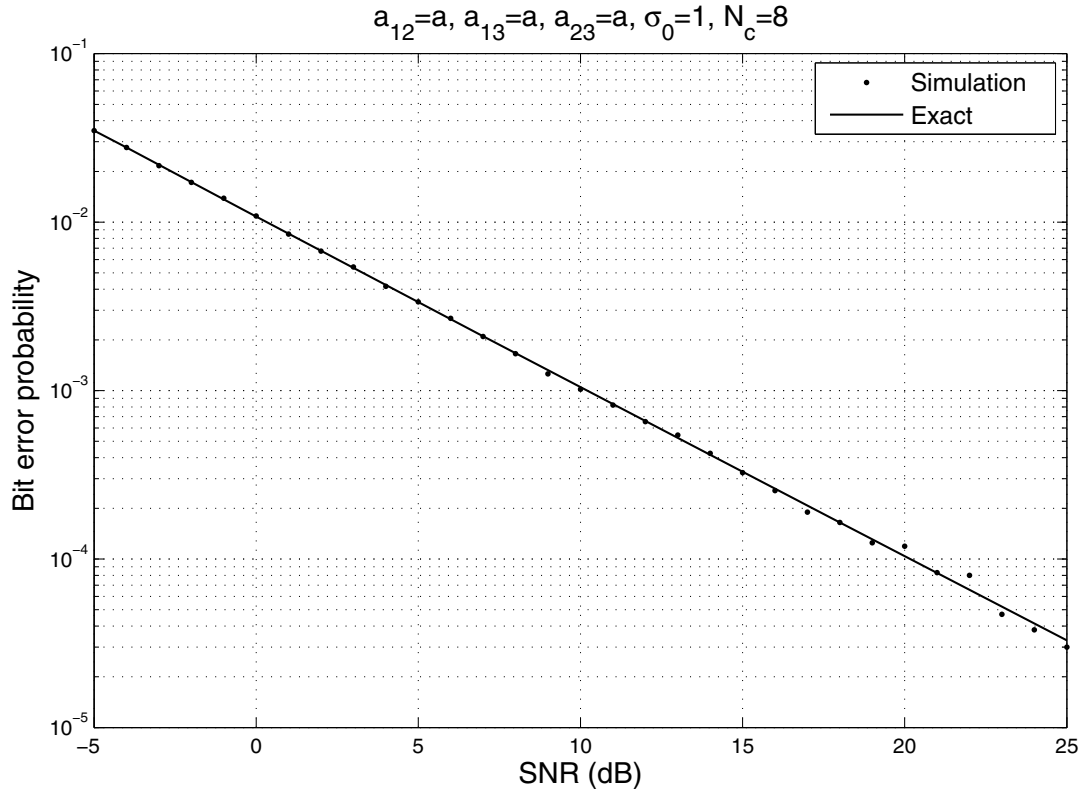
$$U'_1 = N_c \left(K_{10}^2 + (K_{10} + K_{20})^2\right) \tag{35}$$

$$U'_2 = \frac{\sqrt{N_c} \left(2K_{10}^2 - K_{20}^2\right)}{\sqrt{K_{10}^2 + (K_{10} + K_{20})^2}} \tag{36}$$

Considering $D_{u'1}$ as the region of the plane $K_{10} \times K_{20}$ where $N_c \left(k_{10}^2 + (k_{10} + k_{20})^2\right) \leq u'_1$, it can be seen that $D_{u'1}$ corresponds to the area of an ellipse whose center is in the origin (0, 0). Unfortunately, the evaluation of the integral (20) is rather complex for the domain $D_{u'1}$. For this reason, we consider a simplified version of $D_{u'1}$, as being the area of a circle expressed as $k_{10}^2 + k_{20}^2 \leq u'_1$. This simplification can be applied since a circle corresponds to a particular case of the general ellipse. Hence

$$F_{u'_1}\left(u'_1\right) = \int\limits_{k_{20}=-\sqrt{u'_1}}^{\sqrt{u'_1}} \int\limits_{k_{10}=-\sqrt{u'_1-k_{20}^2}}^{\sqrt{u'_1-k_{20}^2}} f_{k_{10}k_{20}}\left(k_{10}, k_{20}\right) \mathrm{d}k_{10}\mathrm{d}k_{20} \tag{37}$$

This gives

$$f_{u'_1}\left(u'_1\right) =$$
$$\int\limits_{k_{20}=-\sqrt{u'_1}}^{\sqrt{u'_1}} \frac{1}{2\sqrt{u'_1-k_{20}^2}} \left\{ f_{k_{10}k_{20}}\left(\sqrt{u'_1 - k_{20}^2}, k_{20}\right) + \right.$$
$$\left. f_{k_{10}k_{20}}\left(-\sqrt{u'_1 - k_{20}^2}, k_{20}\right)\right\} \mathrm{d}k_{20} \tag{38}$$

Figure 3 Comparison of the exact and simulated bit error probability adopting an equal power allocation scheme with λ = 0.5.

Since K_{10} and K_{20} are independent Rayleigh distributed with parameters α_1 and α_2, respectively, the PDF of U'_1 given in (38) will result in a chi-square probability distribution with four degrees of freedom [8]. Therefore, our approximation of U_1 will be given by

$$f_{u_1}(u_1) \approx \frac{4u_1}{\gamma_1^2} e^{-2u_1/\gamma_1} \qquad (39)$$

where γ_1 is the mean of U_1 given in (14)

$$\gamma_1 = E[U_1] \qquad (40)$$

Figure 4 shows the comparison between our approximate PDF given in (39) and the computer simulation for the PDF of U_1 given in (14) for two different values of λ keeping the same values for $a_{12} = 1$, $a_{13} = 2$, and $a_{23} = 3$. We observe that the curves are very close for both values of λ. Although only these two cases are presented here, many other cases were compared and the approximation still remains very good.

A similar rationale can be applied in order to find a good approximation for U_2. The region of the $K_{10} \times K_{20}$ plane where $U'_2 \leq u'_2$ is similar to (29). Note that the range of U_2' varies from $-\infty \leq u_2' \leq \infty$, discarding all

the distributions with positive support. In order to observe the behavior of the PDF of U_2', a large number of simulations were performed, and the Gaussian distribution proves to fit extremely well in all the cases. Therefore, assuming a Gaussian distribution, the following can be written

$$P_{e_f} \approx \frac{1}{4}\left(1 + \sqrt{\frac{\gamma_{12}}{2 + \gamma_{12}}}\right)\left(1 - \frac{\sqrt{\gamma_1}(\gamma_1 + 6)}{(\gamma_1 + 4)^{3/2}}\right) + \frac{1}{2}\left(1 - \sqrt{\frac{\gamma_{12}}{2 + \gamma_{12}}}\right)Q\left(\frac{\gamma_2}{\sqrt{1 + v^2}}\right) \quad (41)$$

$$f_{u_2}(u_2) \approx \frac{1}{\sqrt{2\pi v^2}} e^{-\frac{(u_2 - \gamma_2)^2}{2v^2}} \qquad (42)$$
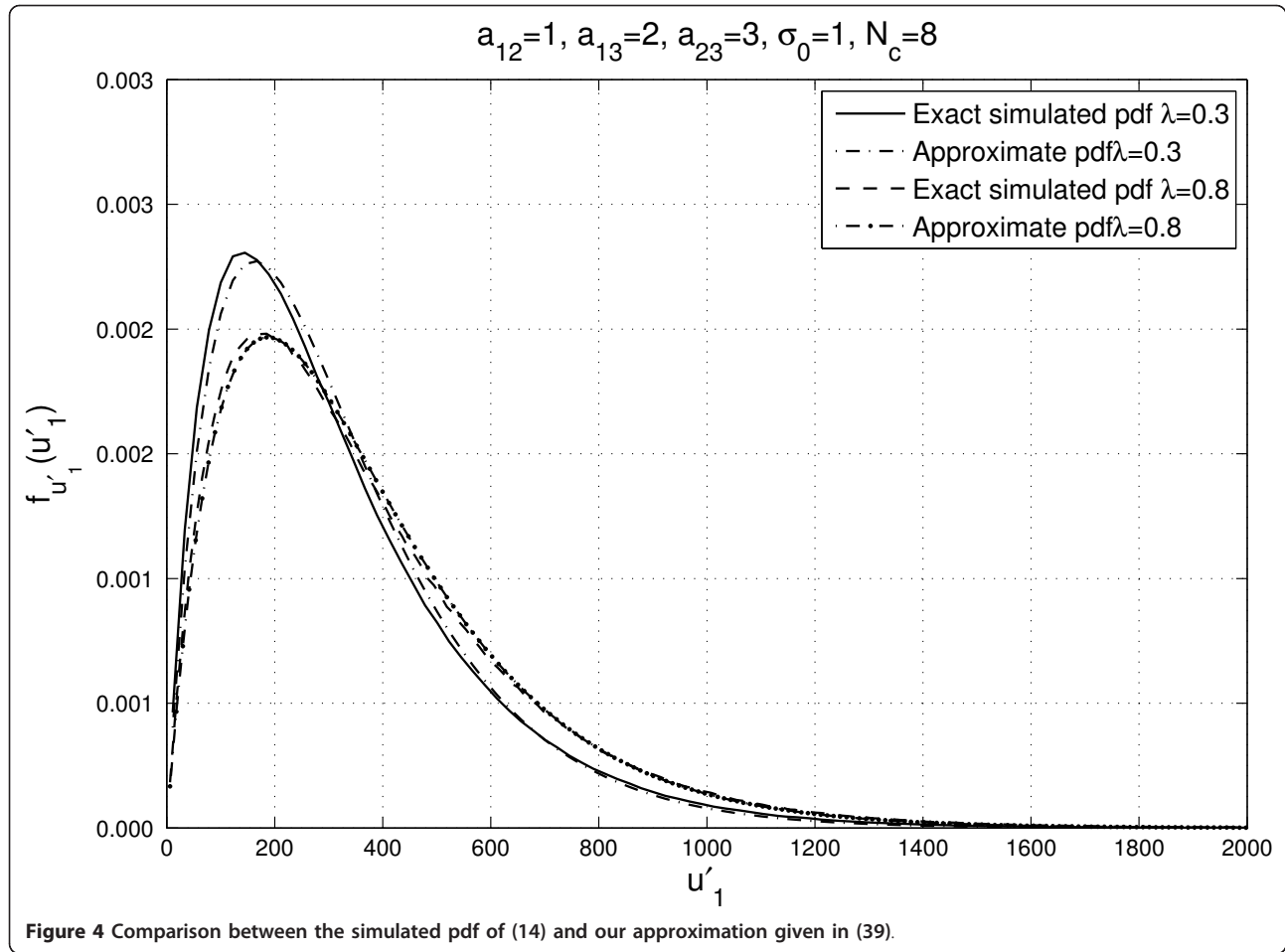
where

$$\gamma_2 = E[U_2] \qquad (43)$$

$$v^2 = \text{var}(U_2) \qquad (44)$$

Figure 5 shows the comparison between the approximate PDF given in (42) and the computer simulation for the PDF of U_2 given in (15), for two different values of λ. Note that the approximation is less accurate for small values of λ, but this inaccuracy does not have a significant influence in the bit error probability. In all

Figure 4 Comparison between the simulated pdf of (14) and our approximation given in (39).

the cases, the approximation fits very well the exact PDF of U_2.

Using (39) and (42) into (17), it is possible to obtain a very accurate approximate bit error probability. Fortunately, both integrals can be found in a closed-form solution as

$$\int_0^\infty Q\left(\sqrt{u_1}\right) \frac{4u_1}{\gamma_1^2} e^{-2u_1/\gamma_1} du_1 = \frac{1}{2}\left(1 - \frac{\sqrt{\gamma_1}\left(\gamma_1 + 6\right)}{\left(\gamma_1 + 4\right)^{3/2}}\right) (45)$$

and

$$\int_{-\infty}^\infty Q\left(u_2\right) \frac{1}{\sqrt{2\pi v^2}} e^{-\frac{(u_2-\gamma_2)^2}{2v^2}} du_2 = Q\left(\frac{\gamma_2}{\sqrt{1+v^2}}\right) (46)$$

All these calculations lead to the approximate bit error probability for the λ-MRC detector as shown in (41), where γ_{12} is given in (13), γ_1 is given in (40), γ_2 is given in (43), and v_2 is given in (44).

Assuming an equal power allocation scheme ($a_{12} = a_{13} = a_{23} = a$), Figure 6 shows the comparison between the theoretical bit error probability presented in (17)
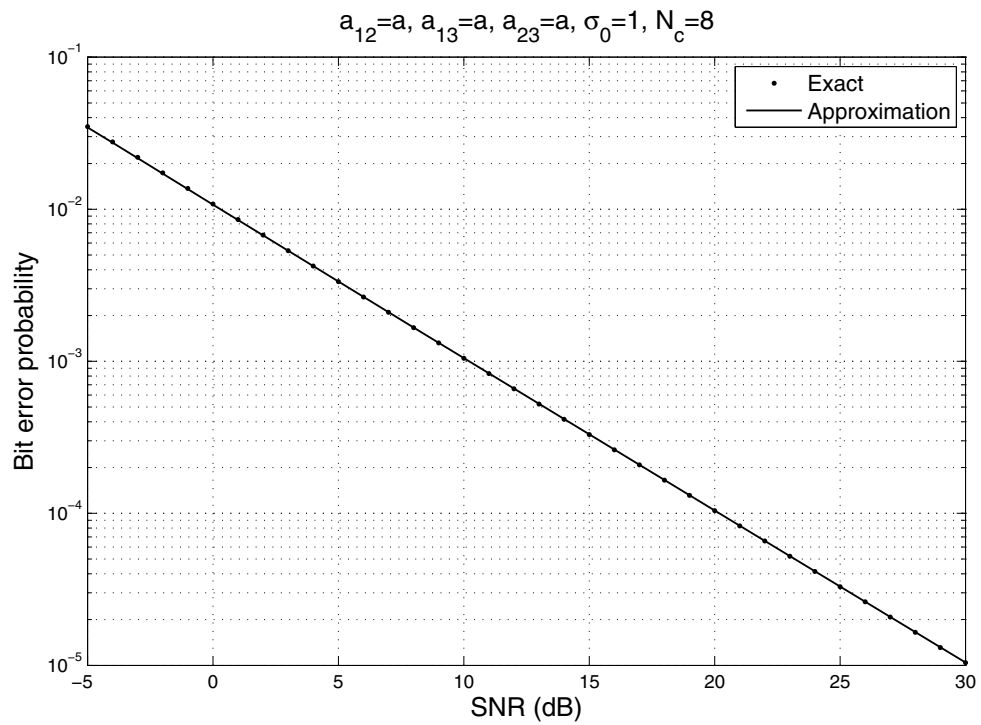
using the exact PDFs (28) and (31) and our approximation given in (41). We can observe that both curves are almost the same, validating our approximation.

Our results are quite exact for a different power allocation scheme as well. This can be seen in Figure 7, where a comparison between the exact simulated bit error probability and our approximation given in (41) was performed. In this figure, the following parameters were used $\alpha_{10} = \alpha_{20} = 1$ and $\alpha_{12} = 0.8$.

The final approximate expression allows us to determine the optimal value for λ in each case. As stated in [1], when the BS believes that the inter-user channel is "perfect", then λ = 1 and the optimal detector turns out to be the maximal ratio combining [7]. As the inter-user channel becomes more unreliable, i.e., as $P_{e_{12}}$ increases, the value of the best λ decreases toward to zero. In order to demonstrate this behavior, Figure 8 shows the optimized λ* versus the inter-user channel parameter α_{12}. This curve was obtained using computational optimization techniques that minimizes our approximate bit error probability (41) with respect to λ for each value of the inter-user channel parameter, α_{12}. The direct
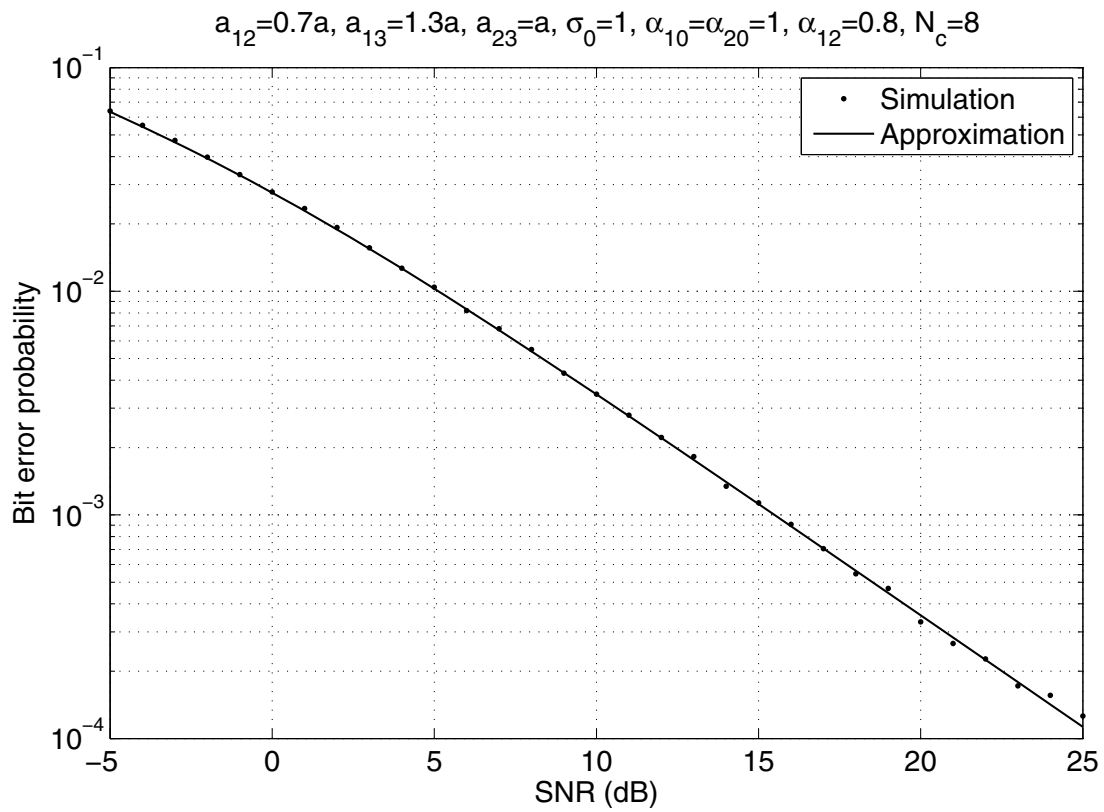
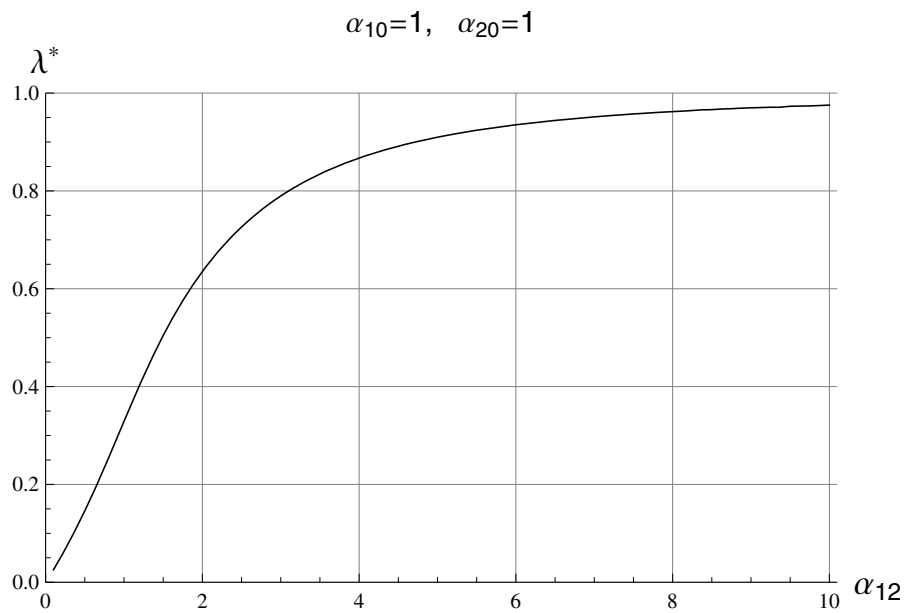**Figure 5 Comparison between the simulated PDF of (15) and our approximation given in (42).**

Figure 6 Comparison between exact and approximate bit error probability using an equal power allocation scheme with $\lambda = 0.5$.

Figure 7 Comparison between exact and approximate bit error probability for a non equal power scheme allocation λ = 0.5.

Figure 8 Optimized λ* versus α_{12}.

channel parameters $\alpha_{10} = \alpha_{20} = 1$ were kept constant, and the equal power allocation scheme ($a_{12} = a_{13} = a_{23} = 1$) was adopted.

IV. Conclusions

In this paper, an exact and approximate expression for the average bit error probability under Rayleigh fading for the λ-MRC presented in [1] was obtained.

The exact expression was obtained under the condition of an equal power allocation scheme. The expression was validated through simulations showing a perfect agreement between exact and simulated curves.

In order to reduce the complexity of the exact expression, a very accurate approximation was presented as well. The approximate expression is valid for any values of λ, a_{12}, a_{13}, and a_{23}. The expression has been validated by simulation for a variety of values showing a small difference between the exact and approximate curves.

Both expression can be very important in many situations where the performance of a cooperative system employing CDMA should be evaluated.

V. Competing Interests

The authors declare that they have no competing interests.

Appendix

$$R_1 = 2M_1 + M_2 + \frac{M_3}{M_2}$$

$$R_2 = 24k_{20}\lambda^2\mu_2^2 A_2\lambda_1\sqrt{\frac{3}{R_1}} + 8M_1 - 2M_2 - \frac{2M_3}{M_2}$$

$$M_1 = 2A_2^2\lambda\,\lambda_1 k_{20}^2 + \lambda_2 u_2^2$$

$$M_2 = \sqrt[3]{E + 2\left(G + A_2 k_{20}\lambda\lambda_1 u_2^2\sqrt{27F}\right)}$$

$$M_3 = 16A_2^4\lambda^2\lambda_1^2 k_{20}^4 -$$
$$4A_2^2\lambda\left(2\lambda^3 + 5\lambda^2 + 2\lambda - 1\right)u_2^2 k_{20}^2 + \lambda_2^2 u_2^4$$

$$E = -\lambda_2^3 u_2^6 + 6(A_2 K_{20})^2\lambda\lambda_5 u_2^4 -$$
$$24(A_2 K_{20})^4\lambda^2\lambda_1^2\lambda_3 u_2^2$$

$$F = -16(A_2 k_{20})^6\lambda^2\lambda_1^2\lambda_4 + 8(A_2 k_{20})^4\lambda\lambda_7 u_2^2 -$$
$$(A_2 k_{20})^2\lambda_6 u_2^4 + \lambda_2^3 u_2^6$$

$$G = 32(A_2 k_{20})^6\lambda^3\lambda_1^3$$

$$\lambda_1 = \lambda + 1$$

$$\lambda_2 = \left(\lambda^2 + 1\right)$$

$$\lambda_3 = \left(2\lambda^2 + 3\lambda - 1\right)$$

$$\lambda_4 = \left(5\lambda^2 + 2\lambda + 1\right)$$

$$\lambda_5 = \left(2\lambda^5 + 5\lambda^4 - 5\lambda^3 - 14\lambda^2 - 7\lambda - 1\right)$$

$$\lambda_6 = \left(13\lambda^6 + 28\lambda^5 - 34\lambda^3 - 12\lambda^2 - 8\lambda + 1\right)$$

$$\lambda_7 = \left(7\lambda^5 + 22\lambda^4 + 17\lambda^3 + 3\lambda^2 - 1\right)$$

References

1. A Sendonaris, E Erkip, B Aazhang, User cooperation diversity Part II: Implementation aspects and perfomance analysis. IEEE Trans Commun. **51**(11), 1939–1948 (2003). doi:10.1109/TCOMM.2003.819238
2. EC van der Meulen, Three-terminal communication channels. Adv Appl Probab. **3**(1), 120–154 (1971). doi:10.2307/1426331
3. TM Cover, A El Gamal, Capacity theorem for the relay channel. IEEE Trans Inform Theory. **25**(5), 572–584 (1979). doi:10.1109/TIT.1979.1056084
4. A Nosratinia, TE Hunter, A Hedayat, Cooperative communication in wireless networks. IEEE Commun Mag. **42**(10), 74–80 (2004). doi:10.1109/MCOM.2004.1341264
5. JN Laneman, DNC Tse, GW Wornell, Cooperative diversity in wireless networks: Efficient protocols and outage behavior. IEEE Trans Inform Theory. **50**(12), 3062–3080 (2004). doi:10.1109/TIT.2004.838089
6. A Sendonaris, E Erkip, B Aazhang, User cooperation diversity Part I: System description. IEEE Trans Commun. **51**(11), 1927–1938 (2003). doi:10.1109/TCOMM.2003.818096
7. JG Proakis, Digital Communications, 4th ed. (McGraw-Hill, New York, 2001)
8. S A Papoulis, Unnikrishna Pillai, Probability, Random Variables and Stochastic Processes 2001, 4th ed. (McGraw-Hill, 2002)